Construction and calibration of an optical trap on a fluorescence optical microscope

Woei Ming Lee, Peter J Reece, Robert F Marchington, Nikolaus K Metzger & Kishan Dholakia

SUPA, School of Physics and Astronomy, University of St. Andrews, North Haugh, St. Andrews KY16 9SS, UK. Correspondence should be addressed to K.D. (kd1@st-andrews.ac.uk).

Published online 13 December 2007; doi:10.1038/nprot.2007.446

The application of optical traps has come to the fore in the last three decades. They provide a powerful, sterile and noninvasive tool for the manipulation of cells, single biological macromolecules, colloidal microparticles and nanoparticles. An optically trapped microsphere may act as a force transducer that is used to measure forces in the piconewton regime. By setting up a well-calibrated single-beam optical trap within a fluorescence microscope system, one can measure forces and collect fluorescence signals upon biological systems simultaneously. In this protocol, we aim to provide a clear exposition of the methodology of assembling and operating a single-beam gradient force trap (optical tweezers) on an inverted fluorescence microscope. A step-by-step guide is given for alignment and operation, with discussion of common pitfalls.

INTRODUCTION

Optical trapping is a technique that utilizes the momentum of light to immobilize, orient and transport micrometer- to nanometer-sized objects within a fluid medium. The technique was pioneered by Ashkin[1], who identified a number of geometries for using optical forces to levitate and trap dielectric particles. The term optical tweezers[2,3] refers to a particular geometry where a single laser beam is focused through a high numerical aperture (NA) microscope objective (MO) to generate a three-dimensional trapping volume within a sample medium. Optical tweezers can be referred to as a single-beam optical trap. A simple and direct extension of the single-beam optical trap is a dual-beam optical tweezers system that may be formed by splitting a single-beam optical trap into two independent optical traps with polarization optics[4]. The two optical traps have orthogonal linear polarizations that reduce any possible optical interference between them. With a dual-beam tweezers system, one can impose differential forces upon biological macromolecules, for example, DNA strands, by tethering the molecules between two microspheres that are held in each of the two independent traps, each with a variable optical force (see **Supplementary Note 1** online for directions on how to obtain a dual-beam optical tweezers system). The appeal of the single-beam optical trap over other optical trapping techniques lies in its simplicity, robustness and compatibility with modern optical microscopy techniques. A microsphere trapped by optical tweezers can act as a calibrated force transducer[3] with piconewton resolution and nanometer precision. It is a noninvasive quantitative force probe with an operating range that is inaccessible to other techniques (e.g., atomic force microscope). Much of the success of this methodology is highlighted by the diversity of its applications across the spectrum of scientific disciplines, particularly in biology, where it has contributed markedly to our understanding of the biomechanics of cells[5], the dynamics of single biological macromolecules including DNA[6] and the behavior of a variety of motor proteins[7–12].

A popular approach has been to implement an optical tweezers system onto a commercially available research-grade optical microscope[9,10]. An optical microscope has the benefit of having a pre-aligned and robust imaging system that routinely performs traditional methods of high-resolution microscopy (e.g., differential phase contrast, dark field, fluorescence and confocal). It is also an apparatus that is readily available in many biological research laboratories. With well-calibrated optical tweezers (single-beam optical trap) built onto an optical microscope system, one can perform precise optical force measurements upon biological systems, while observing them with these imaging techniques. Although there has been a wide selection of optical trapping review papers over the last two decades[13–17], there have only been a handful of publications aimed at providing detailed technical steps on setting up a simple optical trapping system[18–20]. Smith *et al.*[18] describe the construction of optical tweezers with a visible helium–neon (He–Ne) laser and a non-infinity-corrected MO using a conventional bright-field upright microscope platform. They use a simple drag force calibration methodology for the characterization of their optical tweezers. Bechhoefer and Wilson[19] show how to increase the trapping strength by using inexpensive but high-power laser diodes to generate stronger optical tweezers while using video tracking programs for studying Brownian dynamics of trapped microspheres. More recently, Appleyard *et al.*[20] describe a self-built system that proves adequate in performing both optical force measurements and fluorescence imaging. Improving the precision of the optical force calibration of the optical tweezers has been a significant part in the development of optical trapping[11,16]. A number of detection methods have been developed to improve the technique of optical force calibration, each exhibiting different merits depending upon the application. These techniques include video-based particle tracking[21], position-sensitive detector-based particle tracking[14,16], optical trapping interferometry[22] and the commonly used back focal plane interferometry[23].

This protocol is aimed at guiding a user (novice) in this field toward acquiring the basic knowledge necessary to quickly establish an optical tweezers setup (single-beam optical trap) and calibrate its optical forces within an inverted fluorescence microscope. We present a single-beam optical trapping setup built from off-the-shelf items, a practical step-by-step guide with specific emphasis on the optical arrangements required and an equipment list. Trouble-shooting steps are included so as to avoid common pitfalls in optical alignment, such as optical aberrations and appropriate beam steering lens relay systems. A glossary is added to this protocol (see **Box 1**) to explain some of the nomenclature commonly used in laser optics and optical trapping. The anticipated results help serve as an

BOX 1 | GLOSSARY (IN ALPHABETICAL ORDER)

Airy disk. These are concentric rings formed around a focused beam. The approximate radius of the airy disk, *r*, is a diffraction-limited spot equal to $0.61\frac{\lambda_o}{NA}$, where λ_o is the wavelength of the light, NA is the numerical aperture of the objective. An expanded Gaussian beam well aligned into an MO will produce a symmetrical airy disk that collapses and expands as it undergoes focusing and defocusing.

Astigmatism. This is an effect that depends on the oblique angle of the light beam. Such aberration would cause the light beam to appear elongated and asymmetrical (elliptical) at the focal point. Depending on the angle of the off-axis rays entering the lens, the elliptical profile may be oriented either horizontally or vertically. See **Figure 3a**(iv).

Back aperture. The exit pupil of a lens. The back aperture of an MO refers to the circular aperture stop (exit pupil) located at the back of an MO. In some instances (not always), the position of the back aperture would coincide with the back focal plane of the MO.

Back focal plane. The plane normal to the principal axis of the lens. It coincides with the back focal length of the lens. In a phase contrast MO, the phase contrast ring is located at the back focal plane of the MO (see **Fig. 5a**).

Beam block. An optical element designed to terminate a laser beam with minimal scattering. It is typically rated for either pulsed or continuous wave lasers up to a certain power level. It is also known as a beam stop.

Beam waist. The radius of the Gaussian beam, *w*, where the intensity falls to $1/e^2$ ($\approx$13.5%) of the maximum value (or the electric field drops to $1/e$ ($\approx$37%) of the maximum value) on the beam axis. The divergence or convergence of the Gaussian beam can be measured by an angle which is subtended by the points on either side of the beam axis, where the amplitude of the electric field has dropped by $1/e$.

Charged coupled device (CCD). A CCD is a light-sensitive integrated circuit that captures the intensity of an image and converts it into an electrical signal.

Coma. In this aberration, which depends on the same effects as astigmatism, the monochromatic light beam has the distinct shape of a 'comet'. The coma aberration often arises from off-axis rays. The rays come at an oblique angle, which causes the rays to reach the observation points at an angle. The aberration can result from tilting of the lens or if the optical train is not centered. See **Figure 3a**(iii).

Gaussian beam. A beam profile commonly found in laser optics. The transverse intensity profile at any point along the beam path may be expressed as $I = I_0 e^{\left(\frac{-2r^2}{w^2}\right)}$, where I is the intensity of the beam, I_0 the intensity at the centre of the beam, r the radius of the beam and w the beam waist.

Half waveplate ($\lambda/2$). A birefringent optical element that rotates the polarization direction of linear polarized light.

Immersion oil. This fluid ensures that there is minimal refractive index mismatch between the MO's lens and the coverslip. The mismatch in the refractive index between immersion oil, cover glass and sample medium brings about spherical aberration and thus the broadening of the beam at the focal region.

Infinity-corrected MO. This objective is deemed to have an infinite conjugate. In laser optics, such an objective would generate a diffraction-limited spot from a well-collimated beam entering its back aperture. In imaging optics, such an objective can form a diffraction-limited image at the image plane of a relay lens or tube lens that is placed within the 'infinity' space.

Laser collimator. A type of lens system that converts the light beam into parallel rays. In practice, the collimator helps reduce the angle of divergence of the laser beam over a long distance.

M^2 factor. Measurement that compares the actual laser beam output profile with that of an ideal Gaussian beam (ideal factor is 1:1). A laser beam with an $M^2 < 1.1$ when focused with a high NA MO permits us to achieve a good-quality optical trap.

Numerical aperture (NA). The NA of an MO can be calculated by multiplying the sine of the angle, θ, of the marginal ray coming from the focal point by the refractive index, n, of the medium in which the rays travel. The NA can be increased by using large refractive index medium such as immersion oil. NA = $n\sin(\theta)$

Optical conjugate point or plane. In the optical system, it represents the relay of the information of the full optical signal from one point to another. Thus, one point is relayed onto the second conjugate/reciprocal point through a set of optical lens, such as a 4f arrangement. For optimal laser beam steering, the pivot point of the steering mirror is imaged onto the center of the back aperture of the MO lens by a 4f arrangement.

Optical train. Optical train refers to the overall beam delivery optical system or the physical path occupied by the traveling beam.

Photodiode/photodetector (PD). A semiconductor device that converts the optical signal (optical power) into an electrical signal (voltage). It is often used to monitor changes in the intensity of a light field. A quadrant photodiode (QPD) is made up of four individual photodiode segments arranged in a tiled 2 by 2 array.

Polarization. In a non-polarized monochromatic light beam for a given direction of propagation, the electric fields oscillating in many directions (all of which are perpendicular to the direction of beam propagation). Each of these electric-field vectors can be decomposed into its horizontal and vertical components relative to the orientation of a linear polarizer that the light beam passes through.

Polarizing beamsplitter cube (PBS). A PBS is used to split the monochromatic light field into its horizontal (transmitted) and vertical electric field (reflected by 90°) components.

Principal axis. An imaginary line that is located along the central axis of a lens.

Prism wheel (PW). A prism wheel is often found in most advanced microscope systems where a series of prisms are mounted onto a rotating wheel. The prism reflects and transmits different percentage of the illumination light onto the different viewing ports of the microscope.

BOX 1 | CONTINUED

Spherical aberration. Spherical aberration occurs when the rays going through the center of a lens and those going through the peripheral region of the lens are not brought into focus together. This occurs because the light fields passing near the periphery of the lens are refracted to a greater degree compared to the light going through the center of the lens. A mismatch between the refractive index of the coverslip and sample solution would increase this aberration in the axial direction. Hence a focused beam would tend to broaden axially. This broadening weakens the optical trap in the axial direction. This effect can be observed when the traps are located further away from the output of the MO lens, where the mismatch of water and glass is more obvious. Using a water immersion objective may help reduce the spherical aberrations, as the MO is corrected for refractive index of water. A good exercise is to measure the k_z axial trap stiffness at a different axial position away from the coverslip (see **Fig. 6c**). The drop in the k_z trap stiffness indicates the effect of the spherical aberration on the optical trap[13]. This form of aberration may also occur in the optical train and can be attributed to incorrect telescopic lens distances used in a telescope lens arrangement. It is important to try and make sure that the full beam diameter of the laser beam does not cover more than 80% of the lens. The presence of spherical aberration in the telescope lens arrangement results in a poorly formed Airy disc as seen in **Figure 3a**(ii).

4f arrangement. This is an optical arrangement where two lenses of focal lengths ($f1$) and ($f2$) are placed such that the spacing between them is ($f1 + f2$); this essentially places the front focal plane of the first lens at the same point as the back focal plane of the second lens. Using this arrangement, an image placed at the back focal plane of the first lens is relayed to the front focal plane of the second lens with a magnification (or demagnification) of $f2/f1$.

experimental guide for the user. For illustrative purposes, we make use of commercially available 1-inch optical cage system components (Thorlabs Inc.) and an inverted research-grade optical microscope (TE2000E, Nikon). However, all the techniques described herein may be employed on microscope systems or with opto-mechanical items from other manufacturers to achieve an equivalent performance.

Optical tweezers construction

Typically, continuous wave lasers are used for optical trapping (tweezing). The few key properties that one should look out for when choosing a good trapping (tweezing) laser include the M^2 factor of the laser, its maximum optical power, pointing stability, power amplitude fluctuations and laser wavelength[16]. A high NA MO lens (NA $\geq$ 1.2) is often used to generate a high-quality three-dimensional optical trap. With high NA MOs, the lateral and axial gradient forces in the optical tweezers are optimized to trap an object in three dimensions. Infinity-corrected MOs are the most commonly used, as they offer the highest flexibility in trapping (tweezing) systems. There are high NA oil immersion or water immersion MO lenses: water immersion MOs are known to display much lower spherical aberration than oil immersion[16]. Good-quality optical tweezers are often produced by overfilling the back aperture[16] of a high NA oil or water immersion MO with a Gaussian beam ($M^2 \sim 1.1$); this is so to obtain a diffracted-limited spot. It is worth noting that it is a good practice to perform a double-objective transmission power measurement to obtain an accurate transmission efficiency of the MO for the chosen laser wavelength[13]. Essentially, when the back aperture of the high NA MO is overfilled with a well-collimated Gaussian beam, it is possible to obtain a single-beam optical trap. However, such a beam-delivery system would lack in maneuverability, as the single-beam optical trap can, in this case, only be translated by physically moving the sample chamber within which the trapped particle resides. Hence, a beam-steering lens relay system may be constructed to ensure that one is able to steer a single-beam optical trap across the sample without the collimated beam walking off its position at the back aperture of the MO[24]. The beam-steering lens system relays the image of the steering mirror onto the back aperture of the MO (see **Figs. 1** and **2**). As a result, any tilt (angular adjustment) in the steering mirror will result in a direct lateral translation of the optical tweezers beam spot at the sample plane.

The particle position may be determined by imaging its interference pattern at the back focal plane of a detection objective (DO) onto a quadrant photodiode (QPD)[23]. The QPD is fabricated from a semiconductor material, that is, silicon (Si) or indium–gallium–arsenide (InGaAs). Each material operates over a characteristic wavelength range, that is, 250–1,100 nm for silicon and 1,000–2,000 nm for InGaAs. When tracking optically trapped particles, one can collect or image the forward- or backward-scattered light signals from the trapping (tweezing) beam (or an auxiliary probe beam) onto the QPD. The response of the detector to the appropriate wavelength is critical to both a faster time response and greater position sensitivity[25].

Experimental design

The first section of the protocol (Steps 1–12) makes use of the schematic diagrams (**Figs. 1** and **2**) that act as a guide to planning the arrangement of the delivery optics for the optical tweezers beam. In our setup, the optical train is made up of two parts: a beam expansion telescope that matches the beam size to the back aperture of the objective (see thick-dot box in **Fig. 1**) and a beam-steering lens system (see thin-dot box in **Figs. 1** and **2**) that images the steering mirror onto the back aperture of the MO. The threaded holes on the optical bench may be used to aid the alignment of the optics.

The second section of the protocol (Steps 13–21) describes the steps to optimize the optical alignment so as to achieve a diffraction-limited spot (**Fig. 3a**) and also measure the optical power of the optical tweezers at the sample plane (**Fig. 3b**).

The third section of the protocol (Steps 22–27) illustrates the physical characteristics of a particle when trapped (**Fig. 4**). A mini-protocol in **Supplementary Note 2** online illustrates the steps to make a suitable sample chamber where suspended polystyrene microspheres are dispersed in solution. When choosing a solution in which the polystyrene microspheres are to be dispersed (i.e., deionized water (H_2O) and heavy water (D_2O) for your measurements), it is important to note that the viscosity and density of the solution used can influence the behavior of the microspheres. Using D_2O instead of normal water can help reduce heating effects from an infrared (IR) laser[26].

A microsphere trapped in an optical trap within a viscous medium can be viewed as an over-damped harmonic oscillator that experiences a linear restoring force $F_{i=x,y\text{ or }z}$ toward the center of the trap. This force can be determined from multiplying the stiffness of the

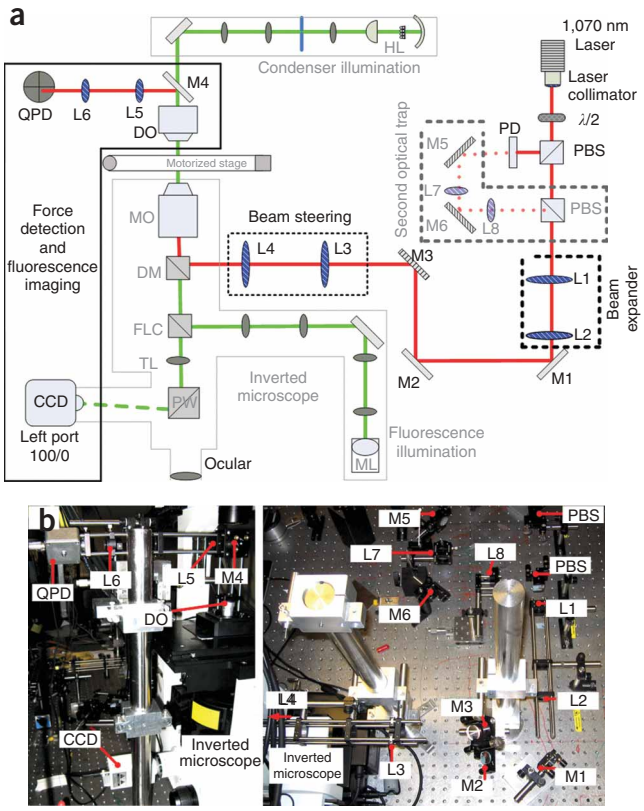

Figure 1 | Experimental setup. (**a**) Schematic of the experimental setup. A collimated laser beam from a 1,070 nm IPG Photonics Ytterbium doped fiber laser, YLM series ($M^2 < 1.1$, maximum optical power of 5 W) is directed onto a half waveplate ($\lambda/2$) to rotate the plane of polarization. Rotating the waveplate before a PBS allows the optical power of the trapping beam to be varied gradually. The power can be measured using a PD. Lenses L1 and L2 are used to form a 6:1 beam expander that expands the collimate beam diameter from 1.6 to 9.6 mm to slightly overfill the back aperture of the MO (diameter ~8 mm). M1 and M2 are broadband IR dielectric mirrors that redirect the beam onto the steering mirror M3. Lenses L3 and L4 form the beam steering lens relay system that images the steering mirror M3 onto the back focal plane of the MO (NA = 1.25) through the infrared DM. The PW is being rotated to output 100% illumination onto the left camera port. DO, IR dielectric mirror M4 and lenses L5 and L6 are used to image the back focal plane from the DO (NA = 0.65) onto the QPD. A CCD camera images the trapped particle in bright-field or fluorescence illumination. A second optical trap (refer to **Supplementary Note 1** online) can be set up using two IR dielectric mirrors M5 and M6, a lens relay system (4f arrangements) using the same focal length lenses L7 and L8 and a PBS (indicated in the gray dotted line). The focal lengths of the lenses are as follows: L1 = 25 mm, L2 = 150 mm, L3=160 mm, L4=160 mm, L5=100 mm, L6= 50 mm, L7=100 mm and L8=100 mm. HL, condenser illumination; ML, fluorescence illumination. (**b**) Photograph of the actual experimental setup (left shows the side view and right photo shows the top view) of the main and second optical traps. Lens L4 (not visible in the photo) is placed to the left of lens L3.

trap, $k_{i\,=\,x,\,y\text{ or }z}$, by the linear displacement of the trapped microsphere ($\Delta i = \Delta x$, Δy or Δz) from the center of the trap. In the last section of PROCEDURE (Steps 28–38), we describe how to implement a back focal plane interferometry-based position-sensing system[23] for calibrating trap stiffness together with fluorescence illumination. One important factor is to calibrate the optical tweezers with highest optical efficiency. To do this, we have chosen to use the interference pattern from the forward-scattered light of a trapped microsphere, generated at the back focal plane of a DO mounted above the sample stage. It is also possible to implement the trap stiffness measurement with the collection of interference pattern from the back-scattered light of the trapped microsphere[27]. The intensity of the back-scattered interference pattern from the trapped microsphere is typically much lower than the intensity of the forward-scattered interference pattern. Hence, it would be beneficial to make sure that the gain on the operational amplifier is optimized for maximum response from the QPD, if the user chooses to make use of the interference pattern from the back-scattered light of the trapped microsphere for calibration of their optical tweezers.

MATERIALS

EQUIPMENT

- Vernier callipers
- Metric/imperial ruler
- Cage system alignment plate with IR card (Thorlabs Inc., part nos. SM1A8 and RMSIR)
- Spirit level

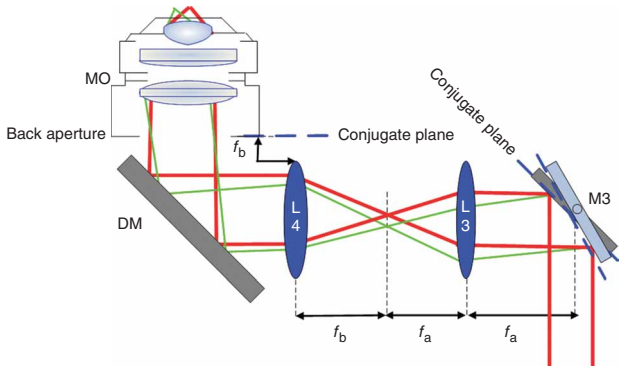

Figure 2 | Beam steering lens relay system. Lenses L3 (focal length f_a) and L4 (focal length f_b) are used for imaging the steering mirror M3 onto the back aperture of the MO. Two sets of parallel laser beams (thick red and thin green lines) are drawn to show that the rays are position-invariant at the conjugate planes.

- Optical power meter (Melles Griot, part no. 13 PEM 001/J)
- IR viewer (optional) (Newport, part no. IRV1-1700)
- Research-grade inverted biological/life science optical microscope (Nikon, TE2000E) with the following components:
  100% left camera viewing port and an epifluorescence port
  Bright-field illumination assembly (halogen bulb)
  Fluorescence illumination assembly (mercury lamp)
  Two rotating filter wheels for filter cubes
  Custom-made filter cube with an ultra-thin dichroic mirror (DM) (e.g., z900dcsp Chroma Technology Inc.) or Hot mirror that reflects the near-infrared trapping (tweezing) laser beam with more than 80% efficiency and transmits visible light
  Additional (STRATUM) epifluorescence port: incorporating the optical trapping (tweezing) beam
  Motorized stage (H117): *X*–*Y* motorized stage with 1 μm accuracy (Prior Scientific)
  Special adaptor mount: Mounting Physik Instrumente (PI) three-axis nano-positioning stage (P-733.3DD) onto Prior Stage (H117) (Einst Technology Pte Ltd.)
  Two Nikon EPlan oil immersion bright-field MOs: NA = 1.25, magnification ×100 and coverslip corrected = 0.17 mm (Nikon) as MO
  Nikon EPlan bright-field MO: NA = 0.65, magnification ×40 (Nikon) as DO
  Nikon CFI_{60} phase contrast MO: NA = 0.65, magnification ×40 (Nikon)
  Red fluorescence filter cube to view red fluorescent polystyrene sphere and transmit NIR (Nikon; Chroma Technology Inc.)
  Digital HAD color camera (Pulnix)

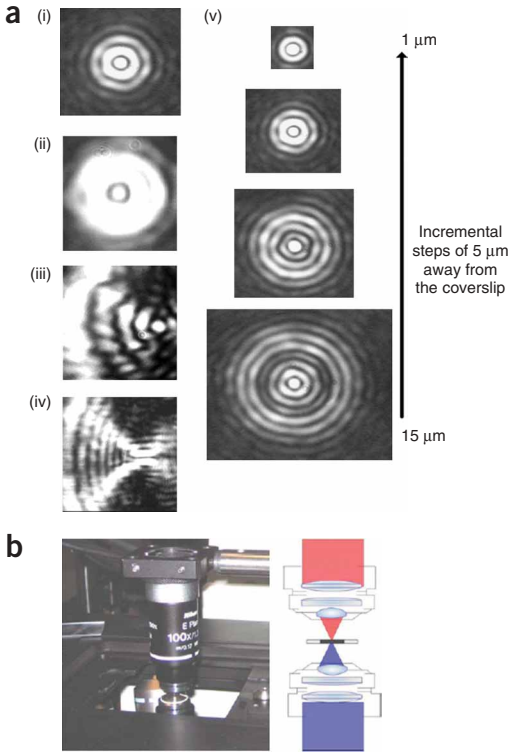

Figure 3 | Airy disk/aberration and power transmission measurements. (**a**) Panel (i) shows the experimental airy disk obtained for an optimal alignment whereas panels (ii–iv) show aberrated beams: spherical, coma and astigmatism, respectively. Panel (v) shows a sequence of images displaying the expanding and collapsing of an airy disk undergoing focusing. Panel (**b**) shows the transmission power measurements with the double objective setup. For the Nikon EPlan oil immersion MO of NA = 1.25, we measured a transmission efficiency of 58% at a wavelength of 1,070 nm.

- Ytterbium-doped fiber laser, YLM series (IPG Photonics) with the following specifications:
  $M^2 < 1.1$
  Output optical power of up to 5 W
  Laser wavelength in the near infrared (1,070 nm)
  Power fluctuations $< 2\%$
  Built-in laser collimator: collimated beam diameter (1.6 mm)
  For laser damage within trapped cells, refer to Neuman and Block[16] and Neuman *et al.*[28]
- Alternative laser suppliers (Coherent; Melles Griot; Koheras; SPi Lasers; JDS Uniphase)
- Optical table with stainless-steel top and threaded holes (Thorlabs Inc.)
- Vibration isolation legs (Thorlabs Inc.)
- Opto-mechanics for mounting freestanding optics and cage assembly, including bases (e.g., BA1), post holders (PH1/M–PH6/M), post (TR20/M–TR300/M) right-angled clamps (RA90/M) (Thorlabs Inc.)
- Three-axis translation stage with manual *x–y–z* micropositioners (Newport, M-562-XYZ)
- RMSA2 external RMS to internal M25 thread adapter to mount Nikon MO onto cage plate (CP02/M) (Thorlabs Inc.)
- High-reflective ($R > 99\%$) NIR dielectric mirrors (BB1-E03) with kinetic mounts (KM100) (Thorlabs Inc.)
- Thorlabs cage assembly system, including cage rods (ER05-ER8) and cage plates (CP02/M) (Thorlabs Inc.)
- Two mounted zero order, half waveplate ($\lambda/2$), 1,064 nm (WPH05M-1064) with rotation mount (RSP1/M) (Thorlabs Inc.)
- Two 1,064 nm polarizing beamsplitter cube (PBS; Newport, 10FC16PB.7) and mount (Newport, UPA-CH1; Thorlabs Inc.)
- BK7 1-inch (25.4 mm) plano-convex lenses with anti-reflective coating in the near infrared (e.g., LA1509-C) (Thorlabs Inc.)

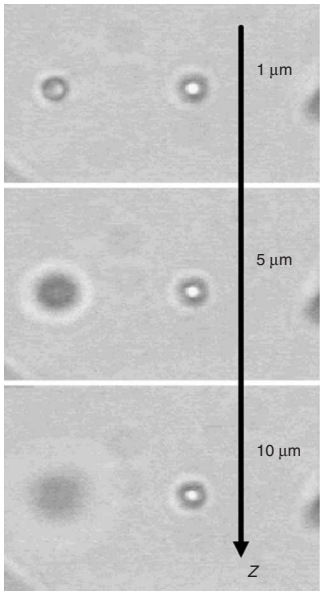

Figure 4 | Three-dimensional trapping of a 1 μm polystyrene sphere. A trapped 1 μm polystyrene sphere (right) is moved to three different depths (1, 5 and 10 μm). The trapped sphere is in constant focus, whereas a neighboring 1 μm sphere stuck (left) on the coverslip moves out of focus.

- 1.5-inch posts (P1.5-P10) and mounting plates (C1501) for elevated optics (Thorlabs Inc.)
- InGaAs-amplified photodetectors (PDA10CS, Thorlabs Inc.)
- Custom-built operational amplifier circuit for each quadrant of the QPD
- ±15 V power supply to drive the QPD amplifiers
- InGaAs PIN quadrant photo-diode (Hamamatsu, part no. G6849)
- Multifunction data acquisition (DAQ) board (PCI-6221), shielded I/O connector block (SCB-68) and shielded cable (SHC68-68-EPM) (National Instruments)
- Labview program for acquiring time series data from the four quadrants, processing the data, calculating the power spectral density and fitting to an appropriate model (National Instruments)
- *X–Y–Z* nano-positioning stage (P-733.3DD) and digital piezo controller (E-710.3CD) (Physik Instrumente)
- Labview program to control the nano-positioning stage for performing the calibration (National Instruments)
- Microscope slides, 76 mm × 26 mm × 1.0 mm (thickness) with low iron clear glass (VWR International)
- Microscope coverslips (type 1), 24 mm × 24 mm × 0.17 mm (thickness) with low iron clear glass (VWR International)
- Custom vinyl stickers as spacers for enclosed cylindrical chamber
- Suspension of polymer microspheres (fluorescent and nonfluorescent) (Duke Scientific; Bangs Labs): 1 μm, 10 ml (1% solid) fluorescent polymer sphere (cat. no. R0100, lot no. 30185), refractive index = 1.59; 1 μm, 15 ml (1% solid) nonfluorescent polymer sphere (cat. no. 4010A, lot no. 28146), refractive index = 1.59
- Standard oil immersion liquid (refractive index ~1.515) (Nikon)
- Sigmacote (Sigma-Aldrich)

EQUIPMENT SETUP

The construction of a single-beam optical trap into an inverted fluorescence microscope is relatively straightforward and requires very little custom fabrication. Most components are mounted with optical supports that are firmly screwed into a vibration damped (floated) optical table. In the presented design, we make use of only a single laser source and a single QPD[25]. The laser source used in the protocol is a ytterbium-doped fiber laser chosen for its emission band (1,070 nm), which generates minimal heating in biological samples[13,28]. Neuman *et al.*[28] have suggested that traps utilizing wavelengths of 870 and 930 nm are most damaging in *in vivo* biological experiments, whereas traps using lasers at wavelengths of 830 and 970 nm seem to be the least damaging. The fiber laser source has an excellent beam quality ($M^2 < 1.1$), which is essential for

achieving a diffraction-limited trapping volume. Several infrared (IR) dielectric mirrors are used to steer the beam onto the epifluorescence port. The use of multiple mirrors is an easy way of accommodating a long optical path on a small bench and obtaining the necessary optical conjugates for beam steering and avoiding beam walk off. Initial optical alignments are critical in obtaining a diffraction-limited spot, Airy disk, which is central to the production of a high-quality three-dimensional single-beam optical trap. The microscope body may be placed near the edge of a floated optical table to allow adequate space to accommodate the optical train setup. The optical trapping (tweezing) beam delivery to the MO is via the epifluorescence port of the microscope. The user may choose to place the optical elements within a black acrylic case with a lid for the purpose of protection from laser beam, exclusion of room lights and reducing the amount of dust settling on the optics. The overall layout of the optical system is illustrated in the schematic shown in **Figure 1a**. **Figure 1b** shows a photograph of the actual setup with labels. The prism wheel (PW) should be adjusted to the appropriate viewing option: 100% light transmission to the left camera port where a charge coupled device (CCD) camera is mounted. A QPD detector is located above the sample stage to receive the forward-scattered signal through the DO. In **Figure 1**, we also include the setup using polarization optics (highlighted as second trap) for creating a second optical tweezers (see **Supplementary Note 1**). The suggested timings for each procedure are meant as a rough guide for the user, assuming that the appropriate equipment is readily available. **! CAUTION** Never use the microscope oculars for direct viewing with the naked eye when the laser tweezers is in use. An appropriate cover must be installed in the binocular microscope head to prevent any laser light from exiting the eyepieces. During optical alignment, always use appropriate laser safety goggles. Consult your department's laser safety officer for further local laser safety requirements.

PROCEDURE

Arrangement of the optical train for the single-beam optical trap ● TIMING 2 h

1| Set the height of the laser collimator such that it is 10–15 cm above the top of the optical bench and aligned along one of the rows of threaded holes. Use an adjustable tilt mount to ensure that the collimated beam runs parallel to the surface of the optical bench; this will greatly simplify the alignment process. It may be useful to make an alignment marker for checking the height of the beam at various points along the beam path.

2| To control the power of the single-beam optical trap, insert a half waveplate ($\lambda/2$) in a rotation mount approximately 10 cm from the exit of the laser collimator followed by a PBS with an aperture of at least 1 cm. Rotating the half waveplate will change the polarization direction of the linearly polarized input beam and thus result in a change in the relative power in each output arm of the PBS. At this point, the user can either use a photodetector (PD) to monitor the optical power stability or terminate the unused PBS output arm with a beam block. (This output can be used to generate a second trapping beam; see **Supplementary Note 1**.)
▲ CRITICAL STEP Use the half waveplate before the first PBS to control the optical power rather than varying the drive current of the laser to improve laser power stability (a laser such as this usually runs close to its specifications when run well above the threshold current).

3| Using the values of the diameter of the back aperture of the MO and the beam waist of the laser (see specifications of the manufacturer or our own measurements), calculate the focal lengths required for a simple two-lens beam expander combination in a 4f arrangement (lenses L1 and L2). The 4f arrangement is used to expand the beam so as to overfill the back aperture of the objective by around 10%. We use lenses L1 and L2 to form a 6:1 beam expander that expands the collimated laser beam from a diameter of 1.6 to 9.6 mm to slightly overfill the back aperture of the MO (diameter $\sim$8 mm).

4| Mount a cage assembly (Thorlabs Inc.) for the two-lens beam expander such that it runs parallel to the surface of the bench with the central axis at the height of the beam. Before inserting the lenses, check that the beam coincides with the principal axis of the optical arrangement along the entire cage assembly. An alignment marker can be formed using an alignment cage plate (part nos. SM1A8 and RMSIR (Thorlabs Inc.)), which can be used to check the centering of the beam as it travels along the principal axis of cage assembly. If the beam and principal axis do not coincide, translate and tilt the cage assembly until the two axes are aligned. Insert the two lenses (L1 and L2) into the cage assembly at a separation equal to the sum of the focal lengths of the two lenses. Finely adjust the separation of the lenses to achieve a collimated beam at the output of the beam expander; the collimation should be tested over at least 1–2 m.
▲ CRITICAL STEP Use a spirit level to ensure horizontal leveling of the cage system only if the optical table has been levelled.
? TROUBLESHOOTING

5| The second part of the optical train will be constructed at a height that coincides with the entry point of the expanded laser beam into the microscope. At this point, it will be easiest to arrange the optics at this new height and then link the two beam paths using a periscope (M2 and M3) and a redirecting mirror (M1). Mount a DM at an appropriate point below the objective remembering that other optics, such as a tube lens and fluorescence filter cubes, may be present. Measure the height from the bench-top to the center of the mirror; this will define the height at which the steering optics (**Fig. 2**) will be placed. We have chosen to mount the DM in a filter cube (z900dcsp, Chroma Technology Inc.), which fits into a secondary filter carousel sitting directly below the objective ('extended stratum' option available on the TE2000E microscope (Nikon)).
? TROUBLESHOOTING

6| Align the microscope body parallel to the rows of threaded holes of the optical bench. Place the cage assembly for the beam steering lens relay system at the height that coincides with the center of mirrors DM and M3, ensuring that the cage is

parallel to the surface of the optical bench and is oriented coplanar to the normal of the mirror (**Fig. 1**). The tilt may be checked using a spirit level (if the table is level) or an alignment marker.

7| Determine the distance between the back aperture of the objective and the position of lens L4; this will dictate the focal lengths used for lenses L3 and L4 in the beam steering lens relay system (4f arrangement). We use lenses with the same focal length for L3 and L4. Place the steering mirror M3 at a distance equal to four times the focal length of lens L4 from the objective back aperture.
▲ **CRITICAL STEP** Placing the lenses L3 and L4 and the steering mirror M3 at incorrect distances will result in a degraded performance of the optical trap upon beam steering.

8| Place mirror M2 below the steering mirror M3 at the height of the laser collimator and orient the mirrors to form a periscope arrangement (see **Fig. 1**). If necessary, use additional mirrors to redirect the expanded beam onto the face of mirror M3 remembering to keep the beam parallel to the table surface and aligned along the rows of threaded holes wherever possible. Note that as the beam is now expanded to the size of the back aperture, it is more prone to clipping at the edge of the 1-inch optics, which will introduce aberrations to the beam and degrade the quality of the optical trap.

9| Use mirrors M2 and M3 to direct the expanded beam along the principal axis of the lenses L3 and L4. Verify that the beam is aligned along the whole cage assembly using the cage system alignment plate.

10| Place lenses L4 and L3 into a 4f arrangement such that the back focal length of lens L4 coincides with the back aperture of the objective and the front focal length of L3 coincides with the position of the steering mirror M3. In this way, the steering mirror is at the optical conjugate of the back aperture of the MO (see **Fig. 2**).

11| Fine-tune the spacing between lenses L4 and L3 to achieve a collimated output at the back aperture of the objective. This may be done by temporarily removing the objective lens and projecting the laser beam over a distance of 1–2 m.

12| Check that the beam remains centered at the back aperture of the MO by tilting the steering mirror M3 over a suitable range of angles. The user may place a marked pointer onto a piece of transparent tape (e.g., Scotch Tape) that is stuck over an empty objective mount and use an infrared (IR) viewer to view the beam. Before steering the mirror M3, the user can check that the beam aligns with the principal axis of the condenser.

Alignment of a diffraction-limited spot for the single-beam optical trap ● TIMING 20 min

13| Adjust the PW to viewing option: 100% left camera port and position a CCD camera (e.g., Digital HAD Color CCD Camera (Pulnix)) at the port. This viewing configuration enables bright-field and fluorescence imaging.

14| Place a clear microscope glass slide on the sample holder of the motorized stage and adjust the microscope focusing knob until Airy disks are observed from the (~4%) back-reflected light of the microscope glass–air interface (see **Fig. 3a**(i)). Adjust the fine focus until the size of the Airy disks is minimized. Note that when the image of the trapping beam is first observed at the focus of the microscope, there is a high probability that aberrations will be present because of slight misalignment in the optical train. Assuming that the above procedure is followed and the beam remains relatively close to the principal axis of the optical train, many aberrations may be corrected using a simple iterative procedure (Steps 15 and 16). See **Figure 3a**(ii–iv) for the expected type of optical aberrations, that is, spherical aberrations, coma and astigmatism.

15| Adjust the steering mirror M3 to place the observed Airy disks to the center of the field of view.

16| Also adjust mirror M2 in tandem with M3 until the Airy disks appear symmetric (see **Fig. 3a**(v)). It may be useful to vary the fine focus of the microscope to observe the symmetry of the Airy disks as they expand and contract. Take notice of any beam asymmetry. Note that you may not be able to achieve a perfectly symmetric pattern on the first iteration (see **Fig. 3a**(ii–iv)).

17| Repeat Step 16 until the beam is centered in the field of view and exhibits a circularly symmetric Airy disk pattern that expands and contracts when the fine focus of the microscope is adjusted (see series of images in **Fig. 3a**(v)).
? TROUBLESHOOTING

Characterization of the power at the focus ● TIMING 30 min

18| Measure the power of the laser at the exit of the laser collimator and passing through the objective mount (temporarily remove the MO). The ratio of the powers is equal to the transmission losses through the optical train.

19| Place an adjustable diaphragm in the objective mount and set the aperture to correspond to the diameter of back aperture of the objective. Measuring the power with and without the diaphragm will provide an estimate of the transmission loss due to overfilling of the back aperture.

20| Prepare a sample of deionized water or D_2O without any microspheres between two type-1 coverslips (thickness ~0.17 mm) (see **Supplementary Note 2** for technique of sample preparation) and mount it on the microscope stage. Gently place a small drop (~20 µl) of immersion oil (refractive index, $n \sim 1.515$) such that it covers the entire area of the front lens of the MO. Slowly move the objective to come into contact with the type-1 coverslip. Vary the focus of the microscope to locate the top and the bottom of the chamber (Airy disks are observed as the focus passes through the water–glass interface). Adjust the position of the focus such that the tweezing beam is placed approximately at 1–2 µm away from the bottom coverslip. The user may choose to use D_2O to reduce heating effects from the IR laser[26]. At this point, the user should maintain the same type of solution to suspend microspheres in for the rest of the steps.

21| Mount a second identical infinity corrected MO (same NA) in an upright orientation, opposing the inverted objective (see **Fig. 3b**). Gently place a small drop (~20 µl) of immersion oil (refractive index, $n \sim 1.515$) onto the top of second MO and gradually move the second objective to come into contact with the top coverslip. Align the upright objective such that the beam coming out of the back aperture is collimated (an *x–y–z* translation stage will aid the alignment). The square root of power loss through the double microscope arrangement (see Step 2) is equal to the transmission loss of one of the MOs. For the E Plan Achromat oil immersion MO of NA = 1.25 (Nikon), we measured a transmission efficiency of 58% at a wavelength of 1,070 nm.
? TROUBLESHOOTING

Trapping a single polystyrene sphere ● TIMING 30 min

22| Prepare a sample containing a dilute concentration of 1 µm polystyrene spheres (see **Supplementary Fig. 1** and **Supplementary Note 2** online) and mount it on the microscope stage with the immersion oil placed on the MO. A typical sample concentration is made by a solution containing 1:1,000 dilution of 1% solid (dilute with deionized water (H_2O) or heavy water (D_2O)).
▲ CRITICAL STEP Too many particles in the sample can lead to undesirable effects when aligning and calibrating the single-beam optical trap, for example, simultaneous trapping of multiple particles or difficulty in moving a single trapped particle within the sample chamber.

23| Set the power of the laser to correspond to approximately 15 mW at the focus. Observe the light scattered from the coverslip–water interface and ensure that it is free from aberration. If this is not the case, follow the procedure outlined in Steps 15–17 to achieve a diffraction-limited spot.

24| Adjust the focus such that the trap center is approximately 5–10 µm from the bottom surface of the chamber; you may still be able to observe defocused Airy disks, which you can use to locate the lateral position of the single-beam optical trap. Move the stage until a polystyrene sphere is in the center of the field of view and then use the steering mirror M3 to position the trap close to the polystyrene sphere (~1–2 µm). The polystyrene sphere will be influenced by the presence of the laser; the response may be characterized by the following observations: (i) The polystyrene sphere will 'hop' toward the beam and become localized at the beam focus (Brownian fluctuations will be suppressed). This indicates that the laser is successfully trapping. (ii) The sphere is trapped in the beam but appears out of focus. This indicates that the trapping (tweezing) plane and the imaging plane are not coincident. (iii) Polystyrene spheres are pushed out of the focus toward the top surface of the chamber.
? TROUBLESHOOTING

25| Lateral trapping (tweezing) can be confirmed by moving the steering mirror M3 and observing the lateral motion of the sphere. Axial trapping (tweezing) can be observed by moving the axial position MO. At all times, the image of the microsphere should stay in focus. See the example reported in **Figure 4**, where a stuck particle is used as a reference.
? TROUBLESHOOTING

26| If the trapped sphere is out of focus, adjust the separation between lenses L1 and L2 so that the trapping (tweezing) plane and imaging plane become coincident. This will introduce a slight convergence or divergence in the beam that is projected at the objective back aperture, which will change the axial positioning of the trap.
▲ CRITICAL STEP Avoid adjusting the positions of L3 and L4 as they are critical to the steering lens arrangements.

27| A simple way to test the quality of the trap before using the QPD force detection system is the *Q* values test[29] (see **Supplementary Note 3** online). In this test, the sample is moved at a different constant velocity using a motorized stage. This in turn creates a Stokes drag force (laminar flow) on the trapped 1 µm polystyrene microsphere. At a certain velocity, the trapped particle escapes from the trap. At this instance, the drag force just surpasses the applied optical force. That velocity is also known as the escape velocity. The applied drag creates an external force F_{drag} that is approximately equal to the applied optical force F_{escape} upon reaching escape velocity. The *Q* values provide an estimate of the quality of the trap.

Setting up and alignment for position-sensitive detection system ● TIMING 2 h

28| Check the fluorescence filter cubes (FLCs) for the appropriate optics (DM, emission filter and excitation filter). At this juncture, consider reading **Supplementary Note 4** online.

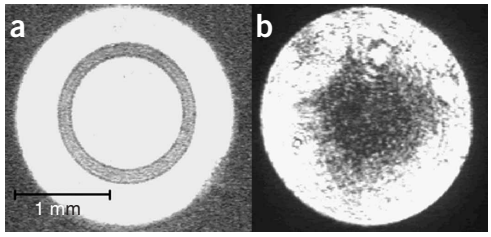

Figure 5 | Phase contrast ring and back focal plane interference. Images obtained using an auxiliary CCD camera showing (**a**) the image of the phase contrast ring using a phase contrast MO with illumination from the fluorescence light. (**b**) The intensity pattern (IR laser) of the back focal plane interference from a trapped 1 μm fluorescent polystyrene sphere. The phase contrast ring of a phase contrast MO assists the user in locating the back focal plane of the bright-field MO. The phase contrast and bright-field MOs should have the same NA.

29| Ensure that the FLC transmits in the spectral bands used for fluorescence excitation and emission. Check that the DM has greater than 80% reflectivity at the trapping (tweezing) wavelength.

30| Remove the Nikon LWD condenser from condenser assembly. Construct an image relay system (L5 and L6) aligned toward the back aperture of a phase contrast MO placed in the position of the DO that is placed above the microscope sample stage see **Figure 1b**, left panel. Ensure that the focal lengths for lenses L5 and L6 are chosen to demagnify the image of the phase contrast ring to fit the size of the active area of the QPD detector.

31| Switch on the mercury lamp (ML) to activate the fluorescence illumination. Illuminate a phase contrast MO placed in the position of the DO. Direct the fluorescence illumination from the MO into the front of the phase contrast MO. Image the phase contrast ring of the MO onto an auxiliary CCD camera that is placed at the position where the QPD will be positioned.

32| Resolve the phase contrast ring with the help of an auxiliary CCD camera mounted onto an *x*–*y*–*z* adjustment stage. Move L5 and L6 in tandem until the phase ring is at the center of the screen and demagnify the size of the phase ring (seen in **Fig. 5a**) to match the active region of the QPD. Change the phase contrast MO to a bright-field MO (NA = 0.65). The bright-field MO will be used as the DO.

33| Increase the optical power (~15 mW at focus) and trap a 1 μm single fluorescent polystyrene sphere. Try to observe the back focal plane interference pattern (IR light) of the trapped sphere (**Fig. 5b**) on the auxiliary CCD camera.

34| Replace the auxiliary CCD camera with the QPD.

35| Switch on the QPD control box and QPD software. We use our own Labview software to capture the position (*x*, *y* and *z*) time series of the trapped polystyrene fluorescent microsphere (see **Fig. 6a**) and analyze the power spectrum to obtain the roll-off frequency or corner frequency, f_c, that is, the frequency response of the particle motion (see **Fig. 6b** and **Supplementary Note 4**)[25]. In the example, a 1 μm polystyrene fluorescent microsphere is trapped at an applied optical power of 15 mW at an axial position of 5 μm above the coverslip. The roll-off frequency, f_c, value is measured at 561.91 Hz. The sampling rate of the data is set at 50 kHz. The measured trap stiffness in the *y*-direction, k_y, is 31.48 pN μm^{-1}. The user can download a MATLAB program that is written by Tolic-Norrelykke *et al.*[30] to analyze the power spectrum. By measuring the axial trap stiffness k_z at different axial planes (2–16 μm) (see **Fig. 6c**), we can see the gradual drop in the axial trap stiffness due to spherical aberration in the trapping beam.

36| Measure k_y at different optical powers (see **Fig. 7**) so as to ensure the linear dependence of the trap stiffness from the applied optical power.

? TROUBLESHOOTING

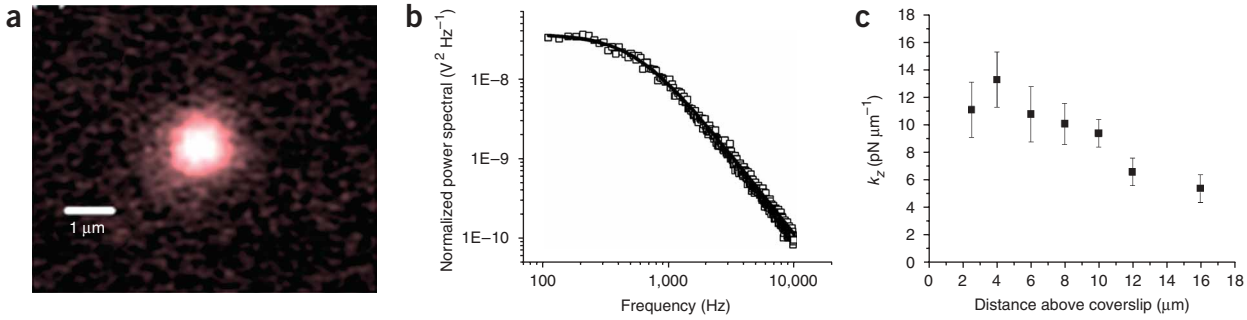

Figure 6 | Trap stiffness for 1 μm red fluorescent sphere. (**a**) Red fluorescence signal from the optical trap. (**b**) Power spectrum for 1 μm polystyrene fluorescent sphere trapped at 5 μm away from the coverslip at an applied power of 15 mW. The trap stiffness in the *y* direction is k_y = 31.48 pN μm^{-1}. The trap stiffness value is determined through the roll-off frequency of f_c = 561.91 Hz. (**c**) The drop in the axial trap stiffness k_z (determined from the roll-off frequency and at a constant applied power of 15 mW) as the trap is moved above the coverslip, due to spherical aberrations.

37| Calibrate the QPD response to nanometer displacements using a nano-positioning stage with a microsphere stuck to the surface of the coverslip: (i) dry out 1 μm microspheres onto a coverslip. Once dry, form a sample chamber and fill with medium (e.g., deionized water or D_2O). (ii) Focus the trapping (tweezing) beam onto one stuck microsphere and position the forward-scattered interference pattern of the stuck polystyrene sphere onto the center of the QPD. Balance the voltage signals from each of the individual quadrants so as to center the interference pattern from the back focal plane of the DO on the QPD. (iii) Translate the nano-positioning stage at nanometer increments such that the beam passes over the stuck sphere. The forward-scattered light from the microsphere at each nanometer increment is recorded as a voltage reading via the QPD. (iv) Map the dependence of the QPD voltage with micrometer displacement (V μm^{-1}) (see **Fig. 8a**). In the example, the linear range is determined by scanning a region of 1 μm by 1 μm and using a step size of 50 nm. We obtain a dependence of 1.27 V μm^{-1}. The linear range of the voltage to displacement dependence can be used to convert the horizontal axis of the position histogram from voltage to micrometers. With the calibrated QPD, the user can determine the average physical displacement of the trapped particle over time $\langle y^2 \rangle^{1/2}$. From our experiment, the half-width of the Gaussian fit of the *y*-position histogram is measured to be approximately 17 nm (see **Fig. 8b**).

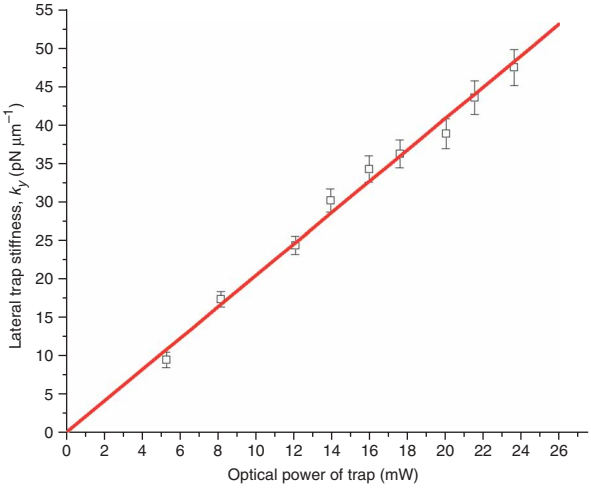

Figure 7 | Linear dependence of trap stiffness determined from the roll-off frequency with optical power of the trap. The lateral trap stiffness varies with the applied optical power in a linear fashion (1 μm fluorescent polystyrene sphere trapped at an axial depth of 5 μm away from the coverslip).

▲ **CRITICAL STEP** It is critical to ensure that the microsphere is properly adhered on to the coverslip surface. Translate the trapping (tweezing) beam with the steering M3 and observe whether the stuck microsphere follows the beam.

38| Use the fluorescence illumination from the ML to image the red fluorescence from the trapped 1 μm single fluorescent polystyrene sphere onto the CCD camera and simultaneously determine the trap stiffness from the roll-off frequency of the power spectrum, f_c, with the QPD (see **Fig. 6a,b**).

? TROUBLESHOOTING

Troubleshooting advice can be found in **Table 1**.

TABLE 1 | Troubleshooting table.

Step	Problem	Possible reason	Solution
4	Expanded beam looks elliptical	Misalignment in the optical setup	Use the cage system alignment plate to check beam centering over the length of the telescope. Avoid using spherical lenses with very short focal lengths (<2.5 cm), as they are more susceptible to introducing aberrations in the optical train if not well aligned
5	Dichroic mirror (DM) displaces image on the CCD camera and/or blocks the fluorescence/bright-field imaging	Loss in the optical power at the sample plane (>50%) and secondary reflection of the beam at the sample plane	Choose a narrowband NIR dichroic mirror with a thin substrate that is transparent to spectral bands used for bright-field and fluorescence imaging (e.g., Chroma Technology Inc., part no. z900dcsp)
17	Observing coma and astigmatism aberrations (see **Fig. 3a**(iii,iv))	(i) Beam misalignment at the beam expander (ii) Beam misalignment at the beam steering lens relay system	(i) Check for misalignment of the beam through the beam expanding telescope (ii) Use mirrors M2 and M3 to re-center the beam on the principal axis of the beam steering lens relay systems
17	Observing spherical aberrations (see **Fig. 3a**(ii))	(i) Beam not expanded to the correct beam waist from the beam expander (ii) Clipping of the beam at the first lens of the beam steering lens relay system	(i) Observe beam profile at the entrance of the beam steering lens pair (ii) Make sure that the full beam waist of the laser beam does not cover more than ~80% of lens L3

TABLE 1 | Troubleshooting table (continued).

Step	Problem	Possible reason	Solution
		(iii) Aberration due to incorrect refractive index of the immersion oil used	(iii) Check for the correct immersion oil for the correct objective
		(iv) Aberration due to mismatch of the coverslip thickness	(iv) Check for correct coverslip thickness. Type-1 coverslip thickness is ~0.17 mm
21	Low power transmission	(i) Stability of the laser emission, back-reflection of laser power and thermal fluctuations of the gain medium can cause the laser power to vary as a function of time	(i) Check the stability of the laser. Use an external power meter or a single photodetector to measure the power of the laser directly at the laser collimator over an extended period of time
		(ii) Low reflectivity of the DM	(ii) Check the reflecting efficiency of the DM
24	Unable to trap polystyrene sphere laterally and axially	(i) Aberrations in the beam	(i) Check for aberrations (see **Fig. 3a**) in the beam; if there are aberrations, then follow Steps 14–17 to achieve a diffraction-limited spot
		(ii) Weakly focused beam	(ii) Check that the beam fills the back aperture of the objective
		(iii) Loss in optical power of Gaussian due to beam clipping	(iii) Check the beam at each of the optics for clipping. If not, follow Steps 1–21 to realign the beam to the principal axis of the optical train
		(iv) A sphere trapped in the beam that appears out of focus indicates that the trapping plane and the imaging plane are not coincident	(iv) Adjust L1 and L2 to change the divergence of the beam, thereby altering the axial position of the trap
	Polystyrene spheres are pushed out of focus toward the top surface of the chamber	(i) Two-dimensional optical trap due to unfilled back aperture of the microscope objective	(i) Check that the beam fills the back aperture of the objective
		(ii) Trap located too far away (~30 μm) from the bottom of the sample chamber. Severe spherical aberration into the beam, which increases as the focus is moved further into the chamber	(ii) Ensure that the trap is inside the chamber and close to the bottom surface
		(iii) Severe spherical aberration due to incorrect refractive index of the immersion oil used	(iii) Check that appropriate Type-1 coverslip thickness is used for the immersion oil MOs (typically a thickness of 0.17 mm for oil immersion)
		(iv) Air bubbles in the immersion oil	(iv) Make sure that the oil immersion medium is free of bubbles. If not, gently clean with lens cleaning tissue and add a fresh drop of immersion oil onto the sample
		(v) Laser power setting incorrect. Too high an optical power of the tweezing beam increases the axial scattering forces, which tends to push polymer spheres toward the top surface of the coverslip	(v) Check that the power of laser has been correctly set. Average trapping power requirement for a 1 μm microsphere is approximately 15 mW at the focus. If excessive power is required for trapping, check the power transmission loss in the optical train, DM and the MO
25	Polystyrene sphere stays trapped only in the lateral direction. Varying the axial position of the MO moves the trapped sphere out of focus	(i) This type of trapping is better known as standing wave traps, where trapping occurs close to a reflective surface (e.g., coverslip)[32]	(i) Ensure that the trap is inside the chamber and close to the bottom surface
36	Low trap stiffness	Weakly focused beam	Check the filling of the back aperture of the MOs by the expanded beam Check the power of the laser (see Step 21)

ANTICIPATED RESULTS

To illustrate the procedure more vividly, we show the sequence of experimental data that researchers and students can obtain by following these procedures. The results, shown in **Figures 3–8**, serve as a guide to the typical observations that one may make. In **Figure 3a**(i) we see an 'ideal' Airy disk and in **Figure 3a**(ii–iv) examples of aberrated beams resulting from misalignment in the optical train. A sequence of images displaying the symmetrical expansion and collapse of an Airy disk pattern (due to focusing) that indicates a well aligned optical train is shown in **Figure 3a**(v). **Figure 3b** shows the arrangement of the double MO setup that is used to measure the transmission efficiency of the optical power. In **Figure 4**, we show the three-dimensional trapping of a 1 μm polystyrene microsphere (Bangs Lab) moving in the axial direction over a depth of 10 μm within a well-aligned optical trap. Motion in the axial direction is achieved by moving the sample stage relative to the fixed trapping position. The trapped sphere remains in focus as a neighboring 1 μm stuck polystyrene sphere moves out of focus. Alignment of the back focal plane onto the QPD can be achieved with the help of the phase contrast ring. **Figure 5a** is the view with a phase contrast MO. The clearly resolved phase contrast ring indicates that the back focal plane of the MO is appropriately imaged onto the QPD; by adjusting the lens arrangement (L5 and L6), the magnification of the image of the ring is adjusted to match the active area of the QPD detector. In **Figure 5b**, we show the back focal plane interference pattern produced by a trapped particle that is projected on to the QPD when the phase contrast objective is replaced with a bright-field objective (NA = 0.65). The phase contrast and back focal plane interference patterns were taken by temporarily replacing the QPD with an auxiliary CCD camera. The QPD records the intensity fluctuations of the back focal plane interference pattern from the trapped 1 μm microsphere (Duke Scientific). The voltage signals from the QPD allow us to track the intensity fluctuation in *x*, *y* and *z* dimensions and we plot the corresponding power spectral density for each axis *x*, *y* and *z*. In **Figure 6a**, we show the trapped 1 μm fluorescent sphere (Duke Scientific) at 5 μm above the cover glass. In **Figure 6b**, we show the corresponding power spectrum, k_y, in the *y* axis using the forward-scattered QPD approach at an applied optical power of 15 mW. In **Figure 6c**, we show the decrease in the axial trap stiffness k_z at different axial depths from 2 to 16 μm above from the coverslip. In **Figure 7**, we show the linear optical power dependence of the trap stiffness k_y. By using a nanopositioning stage, we can map the voltage signal of the forward-scattered interference patterns from a stuck bead onto a micrometer position grid. **Figure 8a** shows the calibration of the voltage response (V) from the QPD over a lateral displacement (μm) using a nanopositioning stage while a stuck polystyrene sphere is scanned over the trapped beam. In **Figure 8b**, we show the typical position histogram of a trapped particle with trapping (tweezing) power of 15 mW at 5 μm above the coverslip. With the information of the lateral distance of the optical trap, $\langle y \rangle$, it would then be possible to measure the optical forces, F_y, with a known trap stiffness, k_y, $F = k_y \langle y \rangle$.

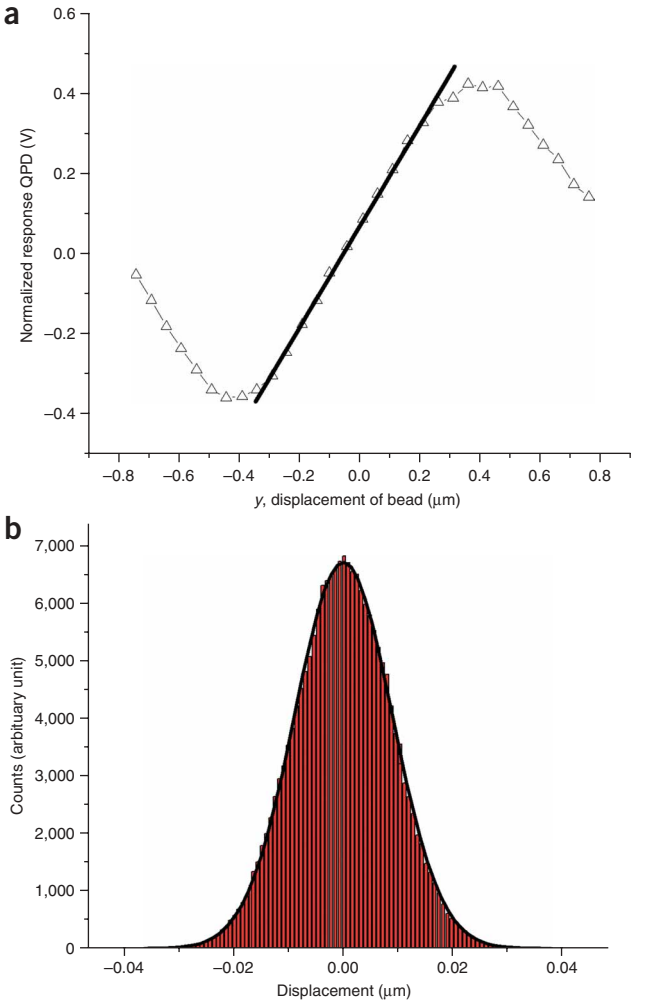

Figure 8 | Voltage response versus *y* displacement and particle position histogram for *y* axis. (**a**) Voltage response versus *y* displacement for *y* axis where the linear range is determined by scanning a region of 1 μm by 1 μm with a step size of 50 nm. The linear dependence was calculated to be 1.27 V μm^{-1}. (**b**) Corresponding histogram of the positions of the 1 μm polystyrene fluorescent sphere at an axial depth of 5 μm in an optical trap with an applied optical power of 15 mW (black solid line—Gaussian fit).

In summary, the optical tweezers system described here can be built with relatively little electronic or optical experience. With a calibrated optical tweezers system, a biologist or a colloidal physicist can measure piconewton forces (or smaller). We have also included a mini-protocol in **Supplementary Note 1**. This describes a direct modification of the single-beam optical trap to create two independent optical traps (tweezers). With such a dual-beam tweezers system, one can make use of the different lateral and axial positions of each of the traps to generate opposing optical forces[31]. This enables studies of the actin–myosin system or those involving stretching of cells and DNA. We remark that several commercial companies offer a range from basic right through to fully automated optical trapping (tweezing) systems: 'Holographic Optical Trapping' from Arryx Inc.,

a portable optical trap or custom trap from Elliot Scientific, 'mmi CellManipulator Automated optical trap' from Molecular Machines & Industries, 'microtweezers' PALM MicroLaser Systems from Carl Zeiss Microsystems. For a more complete bibliography on different aspects of optical traps, we refer the readers to Neuman and Block[16] or Dholakia and Reece[17].

Note: Supplementary information is available via the HTML version of this article.

ACKNOWLEDGMENTS This work is supported by the UK Engineering and Physical Sciences Research Council. We acknowledge several useful discussions with Daniel Burnham.

Published online at http://www.natureprotocols.com
Reprints and permissions information is available online at http://npg.nature.com/reprintsandpermissions

1. Ashkin, A. Optical trapping and manipulation of neutral particles using lasers. *Proc. Natl. Acad. Sci. USA* **94**, 4853–4860 (1997).
2. Ashkin, A., Dziedzic, J.M., Bjorkholm, J.E. & Chu, S. Observation of a single-beam gradient force optical trap for dielectric particles. *Opt. Lett.* **11**, 288–290 (1986).
3. Rohrbach, A. *et al.* Trapping and tracking a local probe with a photonic force microscope. *Rev. Sci. Instrum.* **75**, 2197–2210 (2004).
4. Fallman, E. & Axner, O. Design for fully steerable dual-trap optical tweezers. *Appl. Opt.* **36**, 2107–2113 (1997).
5. Li, Z.W. *et al.* Membrane tether formation from outer hair cells with optical tweezers. *Biophys. J.* **82**, 1386–1395 (2002).
6. Bao, X.Y.R., Lee, H.J. & Quake, S.R. Behavior of complex knots in single DNA molecules. *Phys. Rev. Lett.* **91**, 265506 (2003).
7. Svoboda, K., Schmidt, C.F., Schnapp, B.J. & Block, S.M. Direct observation of kinesin stepping by optical trapping interferometry. *Nature* **365**, 721–727 (1993).
8. Finer, J.T., Simmons, R.M. & Spudich, J.A. Single myosin molecule mechanics—piconewton forces and nanometre steps. *Nature* **368**, 113–119 (1994).
9. Lang, M.J. *et al.* Simultaneous, coincident optical trapping and single-molecule fluorescence. *Nat. Methods* **1**, 133–139 (2004).
10. Tarsa, P.B. *et al.* Detecting force-induced molecular transitions with fluorescence resonant energy transfer. *Angew. Chem. Int. Ed. Engl.* **46**, 1999–2001 (2007).
11. Bustamante, C., Bryant, Z. & Smith, S.B. Ten years of tension: single-molecule DNA mechanics. *Nature* **421**, 423–427 (2003).
12. Bustamante, C., Smith, S.B., Liphardt, J. & Smith, D. Single-molecule studies of DNA mechanics. *Curr. Opin. Struct. Biol.* **10**, 279–285 (2000).
13. Svoboda, K. & Block, S.M. Biological applications of optical forces. *Annu. Rev. Biophys. Biomol. Struct.* **23**, 247–285 (1994).
14. Visscher, K., Gross, S.P. & Block, S.M. Construction of multiple-beam optical traps with nanometer-resolution position sensing. *IEEE J. Select. Top. Quant. Electron.* **2**, 1066–1076 (1996).
15. Lang, M.J. & Block, S.M. Resource letter: LBOT-1: LASER-based optical tweezers. *Am. J. Phys.* **71**, 201–215 (2003).
16. Neuman, K.C. & Block, S.M. Optical trapping. *Rev. Sci. Instrum.* **75**, 2787–2809 (2004).
17. Dholakia, K. & Reece, P. Optical micromanipulation takes hold. *Nano Today* **1**, 18–27 (2006).
18. Smith, S.P. *et al.* Inexpensive optical tweezers for undergraduate laboratories. *Am. J. Phys.* **67**, 26–35 (1999).
19. Bechhoefer, J. & Wilson, S. Faster, cheaper, safer optical tweezers for the undergraduate laboratory. *Am. J. Phys.* **70**, 393–400 (2002).
20. Appleyard, D.C., Vandermeulen, K.Y., Lee, H. & Lang, M.J. Optical trapping for undergraduates. *Am. J. Phys.* **75**, 5–14 (2007).
21. Polin, M. *et al.* Optimized holographic optical traps. *Opt. Express* **13**, 5831–5845 (2005).
22. Svoboda, K. & Block, S.M. Optical trapping of metallic Rayleigh particles. *Opt. Lett.* **19**, 930–932 (1994).
23. Gittes, F. & Schmidt, C.F. Interference model for back-focal-plane displacement detection in optical tweezers. *Opt. Lett.* **23**, 7–9 (1998).
24. Moothoo, D.N. *et al.* Beth's experiment using optical tweezers. *Am. J. Phys.* **69**, 271–276 (2001).
25. Berg-Sorensen, K. & Flyvbjerg, H. Power spectrum analysis for optical tweezers. *Rev. Sci. Instrum.* **75**, 594–612 (2004).
26. Mao, H.B. *et al.* Temperature control methods in a laser tweezers system. *Biophys. J.* **89**, 1308–1316 (2005).
27. Huisstede, J.H.G., van der Werf, K.O., Bennink, M.L. & Subramaniam, V. Force detection in optical tweezers using backscattered light. *Opt. Express* **13**, 1113–1123 (2005).
28. Neuman, K.C. *et al.* Characterization of photodamage to *Escherichia coli* in optical traps. *Biophys. J.* **77**, 2856–2863 (1999).
29. O'Neill, A.T. & Padgett, M.J. Axial and lateral trapping efficiency of Laguerre–Gaussian modes in inverted optical tweezers. *Opt. Commun.* **193**, 45–50 (2001).
30. Tolic-Norrelykke, I.M., Berg-Sorensen, K. & Flyvbjerg, H. MatLab program for precision calibration of optical tweezers. *Comput. Phys. Commun.* **159**, 225–240 (2004).
31. Greenleaf, W.J., Woodside, M.T., Abbondanzieri, E.A. & Block, S.M. Passive all-optical force clamp for high-resolution laser trapping. *Phys. Rev. Lett.* **95**, 208102 (2005).
32. Jonas, A., Zemanek, P. & Florin, E.L. Single-beam trapping in front of reflective surfaces. *Opt. Lett.* **26**, 1466–1468 (2001).